

## Extinction Times in Autocatalytic Systems

Peter D. Drummond,<sup>\*,†</sup> Timothy G. Vaughan,<sup>†</sup> and Alexei J. Drummond<sup>‡</sup>

Centre for Atom Optics and Ultrafast Spectroscopy, Swinburne University of Technology, Melbourne, Victoria, Australia, and Department of Computer Science, The University of Auckland, Auckland, New Zealand

Received: May 17, 2010; Revised Manuscript Received: August 9, 2010

Systems evolving under the influence of autocatalytic processes have been the subject of much study due to their appearance in a wide variety of contexts. Well known examples range from the simplest autocatalytic chemical reactions, biochemical models of ribozyme or prion replication, right up to the duplication of entire organisms in models of population dynamics. While the deterministic approach frequently taken to model such systems is adequate in the limit of large reactant numbers, the intrinsic fluctuations exert an important influence on the dynamics when the supply of reactants is limited. In particular, when combined with spontaneous degradation of the autocatalytic reactant population, such fluctuations can lead to the extinction of that population. In this paper, we study reversible autocatalytic processes of the form  $X + Y \rightleftharpoons 2X$  in the limit that there exists a surplus of  $Y$  and in the presence of a spontaneous degradation process  $X \rightarrow Z$ . Through the use of the Poisson representation, we identify an exact analytical expression for the mean extinction time of the  $X$  population. We show that the exact result can be neatly approximated by an Arrhenius-like expression involving an effective activation energy separating a quasi-stationary state from the extinct state.

### Introduction

Many processes in nature are effectively autocatalytic. Such processes can themselves be series of microscopic chemical processes such as the self-replication exhibited by ligase ribozymes<sup>1</sup> and peptides,<sup>2</sup> self-perpetuating conformational changes such as those known to be exhibited by prions,<sup>3</sup> or reproduction events in biological populations. (There are often strong correspondences between the coarse-grained dynamics of biological systems and those of chemical systems. For an illustrative example, see Witzemann.<sup>4</sup>) Indeed, any system incorporating self-replicating units can be regarded as effectively autocatalytic. As a result, the theoretical treatment of such processes is widely applicable and receives much attention.

In this paper, we wish to consider the effect on a reversible autocatalytic process of spontaneous decay of the catalyst population. Such decay events naturally occur in many real autocatalytic systems: protein structures such as ribozymes and peptides decay, while individual members of biological populations perish. In the absence of a balancing replenishment process, this degradation can lead to the irreversible extinction of the autocatalytic population. Due to the ubiquity of autocatalytic processes in systems of interest and the inevitability of spontaneous decay in many of these systems, we seek to obtain precise estimates of the expected lifetimes of such systems.

We emphasize that the concept of an extinction time of an autocatalytic populations is primarily relevant to autocatalytic systems in which the corresponding uncatalyzed reaction occurs at a far slower rate than the catalyzed reaction. In other words, we focus on systems for which the spontaneous production of the autocatalytic reagent is exceedingly rare over the time scale of the experiment. As a result, this study does not have any particular relevance to autocatalytic models of the origins of

homochirality<sup>5</sup> as uncatalyzed production of each enantiomer occurs easily enough that “extinction” of a given enantiomeric species is usually a meaningless concept. In more complicated biochemical systems, however, the autocatalytic efficiency (i.e., the ratio of the catalyzed rate to the uncatalyzed rate) can be made almost arbitrarily large, with values up to  $10^5$  having been observed in the autocatalysis of certain peptide chains.<sup>6</sup> In these systems, extinction of the autocatalytic population is essentially a one-way event that precludes any real chance of revival.

Much of the original work on reaction dynamics involved rate equations of the form pioneered by Guldberg and Waage<sup>7,8</sup> in which the particulate nature of real populations is replaced by a continuous description. While such deterministic treatments are adequate for large populations (and, due to their relative simplicity, often preferable), extinction events in autocatalytic systems occur only after transition through the small-population regime. For this reason, study of extinction essentially mandates a subtler approach.

For both microscopic chemical systems as well as the more complex composite systems mentioned above, a superior description of the dynamics is provided by the so-called chemical or combinatoric master equation (CME).<sup>9</sup> This describes the time evolution of the probability distribution of the population occupying any one of its accessible discrete configurations. While still an approximation in the sense that the true dynamics may be to some small degree non-Markovian, for many (well-mixed) reacting systems the CME can be regarded as a microscopically accurate description of the stochastic behavior of the system.

The first full stochastic treatment of an autocatalytic process was presented in 1940 by Delbrück,<sup>10</sup> who used a CME to study the intrinsic fluctuations resulting from a linear autocatalytic reaction of the form  $X + Y \rightarrow 2X$  with the  $Y$  population held constant by some external mechanism. This particular CME was found to be exactly soluble and allowed Delbrück to derive an

\* To whom correspondence should be addressed; E-mail: pdrummond@swin.edu.au.

<sup>†</sup> Swinburne University of Technology.

<sup>‡</sup> The University of Auckland.

analytical expression for the time evolution of the probability distribution over the autocatalytic population size.

With only slightly more complex models, however, obtaining exact solutions to master equations (even numerically) is frequently difficult or entirely intractable for realistically sized populations of reagents. This is due to the rapid increase in the volume of the discrete system state space (i.e., the number of all possible population configurations) with the size and diversity of the population. Furthermore, the standard diffusion approximation techniques<sup>11–13</sup> (which seek to alleviate this complexity issue by modeling the discrete stochastic dynamics using continuous diffusion processes) are only valid when the population size remains *consistently* large, a condition clearly violated by systems affected by extinction events. These approximations thus lead to exponentially large errors in calculations of extinction time in well-known stochastic models of autocatalysis.<sup>14</sup>

In this paper we demonstrate that it is possible to derive exact expressions for the mean extinction time of an autocatalytic reactant population through the use of the Poisson representation developed by Gardiner and Chaturvedi.<sup>9,15,16</sup> This approach, which is similar in style to standard generating function methods, involves expanding the discrete probability distribution in terms of an overcomplete basis of Poissonian distributions. For CMEs in particular, the resulting transformed distribution function evolves according to a generalized Fokker–Planck equation (FPE) and can therefore be solved using standard analytical and numerical methods. Our results can be expressed in the familiar form of an Arrhenius expression for the expected time necessary to surmount an effective activation energy barrier that shields the extinct state.

### Basic Model of Autocatalysis with Degradation

The precise mathematical model with which we are concerned consists of a well-mixed system of particles contained within a fixed volume  $V$  and evolving under the influence of two distinct reactions. The first of these is the reversible autocatalytic process



in which  $X$  is the autocatalytic species (both the product and catalyst for the reaction) and  $Y$  is the reagent that is actually consumed in the reaction. On its own, this reaction constitutes the model that has been recently employed by Arslan and Laurenzi<sup>17</sup> to study the effects of intrinsic stochasticity on the dynamics of small autocatalytic systems. In our paper, we assume that the supply of the noncatalytic reactant  $Y$  is so bountiful as to be unaffected by the progress of the reaction. This is the same assumption which was made originally by Delbrück.<sup>10</sup> The above reaction can be replaced with the following effective nonmass-conserving reaction



where we have introduced the rescaled rate constant for the forward reaction  $k'_1 = N_Y k_1$  with  $N_Y$  being the large and approximately constant size of the  $Y$  population.

The second reaction involved in the model is the irreversible degradation or decay process



by which a member of the autocatalytic population spontaneously decays into a nonreacting form  $Z$ . As has already been noted in the introductory paragraphs, such processes often play a role of qualitative importance in the dynamics of many autocatalytic and effectively autocatalytic systems. In particular, in combination with the autocatalytic process given above, spontaneous degradation introduces the possibility that an initially finite number of  $X$  particles may at some later time be completely depleted (driven extinct). As a finite population of  $X$  is necessary to catalyze the replenishment of the population, such depletions are strictly one-way events in this model.

It will be clear to many readers that the general form of the reaction scheme described above is strongly reminiscent of models commonly used in the study of possible autocatalytic origins of the strong homochirality observed in many biological systems.<sup>5,18</sup> For example, the original and simplest such model that was proposed by Frank in 1953<sup>19</sup> includes a pair of enantiomeric populations each participating in separate autocatalytic process similar to that described by forward component of reaction R1. Indeed, the Frank model also incorporates a form of degradation, as the enantiomers are allowed to annihilate one another to form an achiral product that is removed from the (open) system. More recently, models based on studies of the Soai reaction<sup>20</sup> (which formed the first experimental demonstration of an enantiomeric excess arising from autocatalysis) such as the work of Saito and Hyuga<sup>21</sup> emphasize the importance of such degradation or “recycling” in producing strong homochirality, although this particular model has been criticized as being thermodynamically unfeasible.<sup>22</sup>

Despite these superficial similarities, it is important that we reiterate that we do not expect the work presented in this article to be of great interest in the context of studies of enantioselection and the origin of homochirality. This is due to the fact that, as noted earlier, extinction of the autocatalytic population *cannot* be considered a one-way event in such systems. Uncatalyzed production of each enantiomer occurs regularly on a similar (although of course slightly longer) time scale to the catalyzed reaction events.

It is therefore important that we again emphasize that the particular systems we seek to model here are those for which the rate of the reaction  $Y \rightarrow X$  is negligible compared to those of the other reactions in the system. Usual examples of processes that satisfy this requirement of irreversible (or nearly irreversible) extinction are found in models of macroscopic biological dynamics,<sup>23</sup> where the uncatalyzed forward reaction is entropically disfavored due to the quantity of information involved in the replication process. However, it is also the case that many microscopic chemical systems also possess this trait; for example, those involving the replication of ribozymes<sup>1</sup> or peptides.<sup>2</sup> For such systems, which were reviewed by Paul and Joyce,<sup>24</sup> the uncatalyzed forward reaction is significantly suppressed over the time scale of the experiment by improving the efficiency of the catalyzed channel.

Note that description of the parameter space attached to this model can be simplified through the introduction of the composite parameter  $\rho = k'_1/\gamma$ , which is called the birth to death ratio or reproductive ratio in biological applications of the model.

**Rate Equation Description.** The simplest mathematical description of the reduced model incorporating reactions R1' and R2 is given by the following rate equation:

$$\frac{d}{dt}[X] = \gamma(\rho - 1)[X] - k_2 V [X]^2 \quad (1)$$

in which  $[X]$  represents the concentration of the autocatalytic reagent as a continuous and deterministic function of time. This is simply the familiar logistic equation developed by Verhulst<sup>25</sup> as a model of biological population dynamics. In the case that  $\rho > 1$ , the rate equation predicts that the only effect of the decay reaction will be to slow the inevitable climb of the reagent population toward the finite stationary concentration  $[X]_c = \gamma(\rho - 1)/k_2 V$ . The corresponding total particle number is  $N_c = [X]_c V$ . In contrast, for larger decay rates such that  $\rho \leq 1$ , the deterministic description predicts that all initially finite populations will eventually decay to zero.

Additional insight into this description can be obtained by treating the concentration  $[X]$  as a position coordinate in a one-dimensional mechanical system. This system is conservative, as eq 1 can be expressed in the form

$$\frac{d}{dt}[X] = -\frac{\partial U([X])}{\partial [X]} \quad (2)$$

where  $U([X])$  is the following time-independent effective potential,

$$U([X]) = -\frac{\gamma}{2}(\rho - 1)[X]^2 + \frac{k_2 V}{3}[X]^3 \quad (3)$$

which is uniquely defined up to the addition of an arbitrary constant. The dashed line in Figure 1 illustrates the form of this potential for the reaction rates  $k_1' = 10$ ,  $k_2 = 1$ , and  $\gamma = 3$ , for which  $\rho = 10/3 > 1$ . This potential clearly depicts a system with two fixed points: a local maximum at  $[X] = 0$  (unstable) and a global minimum at  $[X] = [X]_c$  (stable). In contrast, the dotted line in the same figure shows the effective potential corresponding to a system for which  $k_1' = 10$ ,  $k_2 = 1$ , and  $\gamma = 10$ . As  $\rho = 1$  in this case, the finite-population fixed point vanishes, causing  $[X] = 0$  to usurp the role of global minimum and become the system's only stationary point.

While providing an accurate description of the dynamics of the system when the concentration of  $X$  is large, the rate equation completely neglects the fundamentally discrete nature of the state space and the corresponding intrinsic stochasticity of the reaction. These factors play important roles in determining whether and, if so, when the autocatalytic population will become extinct. The fundamental issue is that a spontaneous fluctuation can occur such that  $[X] = 0$ . Once this happens, there is no mechanism by which  $[X]$  can increase back to its stationary value. In other words, the stationary concentration  $[X]_c$  is in reality only metastable, while the extinct concentration  $[X] = 0$  is stable.

**Chemical Master Equation Description.** In the chemical master equation description of the model, the concept of a precisely known reagent concentration  $[X]$  is replaced with a time-dependent probability distribution over the possible absolute population sizes of the autocatalytic reagent:

$$\begin{aligned} \frac{\partial}{\partial t} P(n,t) = & k_1'[(n-1)P(n-1,t) - nP(n,t)] + \\ & k_2[n(n+1)P(n+1,t) - n(n-1)P(n,t)] + \\ & \gamma[(n+1)P(n+1,t) - nP(n,t)] \end{aligned} \quad (4)$$

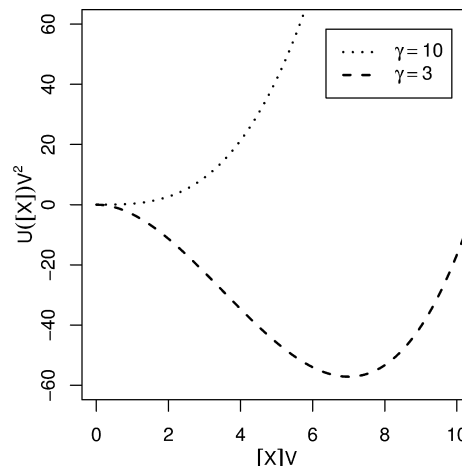


**Figure 1.** Effective potentials governing the dynamics of the deterministic rate equation description of a system with  $k_1' = 10$ ,  $k_2 = 1$  m and both  $\gamma = 10$  (dotted line) and  $\gamma = 3$  (dashed line).

Here we have employed the short-hand notation  $P(n,t) \equiv P(N_X(t) = n)$ , where  $N_X(t)$  is a discrete-valued time-dependent function representing the true (but as yet unknown) path the autocatalytic population will take through its accessible state space.

In the context of extinction times, there is a striking difference between the deterministic rate equation description and the stochastic description provided by the above CME. While the former predicts a true finite-population stationary point for  $\rho > 1$ , the presence of the degradation reaction in the latter yields no strict finite-population stationary point for *any* decay rate. Taking into account the inherent stochasticity in the system thus leads to the conclusion that, for reversible autocatalytic processes, the inclusion of any decay will always lead to extinction.

A related but subtler difference between the two descriptions lies in the fact that the stochastic description allows for the autocatalytic population to become arbitrarily large due to the same stochastic fluctuations that drive extinction events in the  $\rho > 1$  case. While such “runaway” events are at most transient within the confines of the model defined by reactions R1' and R2, it is important to consider that these events may lead to a violation of the simplifying assumption  $N_X \ll N_Y$  upon which the model is based. We will return to this important issue later in the paper.

While no exact analytical solution to the above CME is yet known, approximate solutions to the extinction time problem in equivalent stochastic models have been derived.<sup>23,26</sup> Unfortunately, these earlier results have a rather complex form that is difficult to intuitively interpret.

Alternatively, standard numerical Monte Carlo approaches such as the stochastic simulation algorithm (SSA) developed by Gillespie<sup>27,28</sup> can be used to directly sample times of extinction events from the true distribution. Gillespie's approach involves generating finite numbers of samples from the exact probability distribution via computer simulation. This is restrictive in the sense that the computations become unwieldy for different combinations of model parameters. Despite these complexity issues, the SSA is widely used and, in our case, provides an indispensable means of validating new analytical results.

In discussing the stochastic description of this minimal autocatalytic model, we would be remiss in failing to point out that although our model is not deeply descriptive of the chemical kinetics of chiral autocatalysis, there are undeniable structural similarities between the above CME and those employed in the



many detailed stochastic descriptions of such systems.<sup>29–36</sup> This raises the obvious question of whether or not these existing treatments are relevant to our discussion.

In addressing this question, we first note that none of the models considered in these papers allow for the possibility of the irreversible extinction events that form the focus of this paper and that they are thus unrelated in this important regard. Second, although we appreciate that some of the general approaches used to investigate the dynamics of chiral autocatalysis in these papers are reminiscent of the approaches employed here, none of these investigations utilize the Poisson representation approach, which, as we will demonstrate, is capable of providing exact solutions the extinction time problem.

We draw specific attention to the work of Saito, Sugimori, and Hyuga<sup>33</sup> which, of the papers cited above, is probably the most relevant to the work presented here. They consider the stochastic dynamics of a kinetic model of enantiomeric excess amplification that includes both linear and nonlinear autocatalytic amplification of each of the two chirally distinct populations. These are investigated primarily via analytical analysis of the stationary states of the CME, but also through direct numerical integration and a “directed random walker” Monte Carlo approach. This latter technique is comparable to the Gillespie method used in our paper to verify the results of our analytical analysis but is subtly different due to its reliance on an approximation in which the reactions are assumed to occur at times separated by fixed intervals. In contrast, the event times used in our calculations follow the exponential distribution required by Gillespie’s algorithm, providing results that are provably equivalent to the original CME.

**Poisson Representation of the Master Equation.** A theory exactly equivalent to that provided by the CME in eq 5 above is obtained using the Poisson representation. In this approach, the probability distribution over discrete chemical population configurations is expanded in terms of an overcomplete basis of analytically continued Poissonian probability distributions. That is,

$$P(n,t) = \int d^2x f(x,t) \Lambda(n,x) \quad (5)$$

Here the integral is taken over the entire complex plane and the function  $\Lambda(n,x)$  is an analytic continuation of the Poissonian probability distribution with a mean of  $x$ :

$$\Lambda(n,x) = e^{-x} \frac{x^n}{n!} \quad (6)$$

It is possible to show that there always exists a real, positive-definite distribution  $f(x,t)$  that satisfies eq 5. In fact, due to the overcompleteness of the basis, there are an arbitrarily large number of such distributions; each of which are an exactly equivalent expression of the information contained in the original probability distribution  $P(n,t)$ . Factorial moments can be obtained directly from the transformed distributions via the simple relationship

$$\langle n(n-1)\dots(n-r+1) \rangle = \int d^2x f(x,t) x^r \quad (7)$$

By following a straightforward approach detailed elsewhere,<sup>9</sup> the CME for the model treated in this paper can be transformed into the following equation of motion for the transformed distribution:

$$\frac{\partial}{\partial t} f(x,t) = \left[ -\frac{\partial}{\partial x} A(x) + \frac{1}{2} \frac{\partial^2}{\partial x^2} D(x) \right] f(x,t) \quad (8)$$

where the differential operators act on all terms to their right and we have defined

$$A(x) = \gamma(\rho - 1)x - k_2 x^2 \quad (9)$$

and

$$D(x) = 2k_2 x \left( \frac{k'_1}{k_2} - x \right) \quad (10)$$

This new equation of motion has precisely the same form as that of a Fokker–Planck equation (FPE), which governs the evolution of a probability distribution associated with a continuous-variable diffusion process. This mapping, which is possible for all CMEs describing processes involving no more than two-body reactions, gives the Poisson representation enormous utility; it allows one to turn the vast array of analytical and numerical techniques available for the solution of FPEs toward the solution of these discrete problems. In this new context,  $A(x)$  and  $D(x)$  are referred to as the drift and diffusion terms.

One unique advantage of FPEs over CMEs is that the continuous diffusion described by the former can be equivalently represented by a set of stochastic differential equations (SDEs). In the case of eq 8, the corresponding Itô SDE is

$$dx = [\gamma(\rho - 1)x - k_2 x^2] dt + \sqrt{2k_2 x \left( \frac{k'_1}{k_2} - x \right)} dW(t) \quad (11)$$

where  $dW(t)$  is the Wiener increment for which  $\langle dW(t) \rangle = 0$  and which satisfies the autocorrelation relation  $\langle dW(t) dW(t+\tau) \rangle = \delta(\tau) dt$ . (The angle brackets  $\langle \dots \rangle$  are used here to represent statistical averages over the ensemble of stochastic realizations.)

Note that with the omission of the second term (the noise term), eq 11 becomes identical to eq 1, the standard deterministic logistic model for the progression of the autocatalytic process, with the finite stationary population size  $x_c = N_c$ . It is thus evident that, in the Poisson representation, this noise term accounts for both the discrete nature of the problem and the intrinsic stochasticity which results from this nature.

It is important to again consider that the SDE obtained here via the Chaturvedi–Gardiner Poisson representation is fundamentally different from that which can be obtained by standard approximations such as those due to Kramers and Moyal<sup>11,12</sup> or the system size expansion due to van Kampen,<sup>13</sup> although the stochastic equations generated by these different approaches may bear some similarities to one another. As briefly mentioned in the introductory section, SDEs obtained via these approximate approaches are only valid in the large population limit (i.e.,  $n \gg 1$ ) and are thus useless for the study of fluctuation-driven extinction events such as those forming the focus of the present article, as such events can occur only following a transit of the small-population regime.<sup>14</sup> In contrast, the SDE above was derived without need for any approximation and can be used to exactly calculate moments of the probability distribution at any time, regardless of the population size:

$$\langle x(t)^r \rangle = \sum_n P(n,t) n(n-1) \dots (n-r+1) \quad (12)$$

Equivalently, the full probability distribution can be reconstructed using the relationship

$$\left\langle e^{-x(t)} \frac{x(t)^n}{n!} \right\rangle = P(n,t) \quad (13)$$

Finally, we also note that attempts to treat the inherent stochasticity in this model through the ad hoc incorporation of noise terms into the traditional rate equation description can perform no better than the described systematic approximate approaches, as to proceed in this fashion is to ignore the discrete nature of the real chemical population. This is the same approximation that forms the basis of the mathematically rigorous diffusion approximations already discussed and which breaks down in the study of extinction events.

**Specification of Initial Conditions.** Recall that in presenting a stochastic model of the system dynamics we are admitting a certain degree of ignorance with regard to the microscopic details of these dynamics. Explicitly folding such ignorance into the dynamical model allows us to eliminate the bias that would otherwise be present in our results if we were to base our calculations on unfounded assumptions regarding these unknown details.

For the same reason, it is important to consider that in any real experiment there will be additional sources of uncertainty due to the practical limitations of the reaction preparation method. In particular, the exact number of reactant molecules loaded into a reactor will likely vary substantially between different runs of the experiment, resulting in an overall uncertainty with respect to the initial autocatalytic population size. Although the exact nature of this uncertainty will undoubtedly depend on the details of the apparatus involved, we can make progress by considering that

1. the number of particles equilibrating in a small volume coupled to a large reservoir, i.e., that yielded by the Grand Canonical Ensemble of statistical mechanics, is specified by a Poissonian probability distribution over possible population sizes, and that

2. the number of particles sampled by selecting a small volume from a much larger volume is also subject to a Poisson distribution.<sup>37</sup>

It is therefore natural to expect that even the most exacting means of preparing the autocatalytic population will result in knowledge of the initial number of reactant particles only up to the Poisson probability distribution

$$P(n,0|x_0) = e^{-x_0} \frac{x_0^n}{n!} \quad (14)$$

with only the mean value  $x_0$  being under the control of the experimenter. This approach has precedent in (for example) the work of Voituriez et al.<sup>38</sup> and that of Gopich and Szabo.<sup>39</sup>

### Mean Extinction Times

The problem of calculating the mean extinction time of a stochastically varying chemical population is a specific example of a large class of problems known as first-passage time problems. These involve determining how long on average a random variate takes to reach some boundary. In particular, first-

passage problems involving Fokker–Planck or diffusion processes are ubiquitous in statistical physics and extensive literature exists detailing their solution. In this section we demonstrate that the Poisson representation allows us to turn these existing techniques, with only slight modification, toward the solution of the extinction problem in the discrete stochastic model of autocatalysis—a problem outside of the traditional domain of these methods.

As an aside, we note that Pasquale and Mecozzi<sup>40</sup> have employed the Poisson representation in their calculations of first passage times for a population in the midst of a Malthusian explosion. This is similar to the problem we address here in the sense that the chemical kinetics of their explosion model are the reverse of those described by reactions R1' and R2, but with  $k'_1 = 0$ .

**Exact Results via the Poisson Representation.** For the reasons discussed above, we begin by considering a population of the autocatalytic reagent X with an initial Poissonian distribution of sizes of mean  $x_0$ , as defined by eq 14. In terms of the Poisson representation, this requirement takes the form of the simpler initial condition on the transformed distribution

$$f(x,0|x_0) = \delta(x - x_0) \quad (15)$$

As mentioned earlier, the mapping from Poisson representation distributions to probability distributions is many to one and therefore this expression for the initial distribution is not unique. However, this particular expression has the desirable effect of confining the dynamics of the distribution to the subset  $[0, x_m)$  of the real axis, where  $x_m = k'_1/k_2$ .

After reactions start to occur, it is inevitable that in each realization the population will become extinct at an unknown future time. Due to the irreversibility of these events, the probability  $\mathcal{C}(t|x_0) = P(0,t|x_0)$  that the population is extinct at some time  $t$  is also the probability that the extinction time has already occurred.

The rate of extinction per unit time at time  $t$  given an initial Poissonian with mean  $x_0$  is denoted  $\mathcal{P}(t|x_0)$ . There is always a finite probability that extinction has occurred, equal to  $e^{-x}$ , in a Poisson population of mean equal to  $x$ . Thus, the extinction rate is also proportional to the rate of change of the Poisson distribution conditioned to an initial mean value of  $x_0$ :

$$\begin{aligned} \mathcal{P}(t|x_0) &= \frac{d}{dt} \mathcal{C}(t|x_0) \\ &= \frac{d}{dt} \int_0^{x_m} f(t,x|x_0) e^{-x} dx \end{aligned} \quad (16)$$

Clearly,  $\mathcal{P}(t|x_0) dt$  is just the probability for extinction in a small time interval  $dt$ . That is,  $\mathcal{P}(t|x_0)$  can be regarded as the extinction time probability density function. Hence, the average time to extinction  $T$  given an initial Poisson distribution at  $x_0$  is a weighted time integral over the probability for extinction in each time interval:

$$\begin{aligned} T(x_0) &= \int_0^\infty t \mathcal{P}(t|x_0) dt \\ &= \int_0^\infty t \frac{d}{dt} \mathcal{C}(t|x_0) dt \\ &= - \int_0^\infty t \frac{d}{dt} \mathcal{C}(t|x_0) dt \end{aligned} \quad (17)$$

Here we have introduced a survival probability defined as

$$\begin{aligned}\mathcal{J}(tx_0) &= 1 - \mathcal{E}(tx_0) \\ &= \int_0^{x_m} f(t, x|x_0)[1 - e^{-x}] dx\end{aligned}\quad (18)$$

The absorbing state at  $x = 0$  means that the distribution decays to a delta function at long times:  $f(\infty, x|x_0) = \delta(x)$ , so that

$$\lim_{t \rightarrow \infty} t \mathcal{J}(tx_0) = 0 \quad (19)$$

This last result allows a further simplification from integration by parts, so that

$$T(x_0) = \int_0^\infty \mathcal{J}(tx_0) dt \quad (20)$$

Since  $f(t, x|x_0)$  is a normalized, probabilistic propagator function in the Poisson representation, this leads to a simple prescription for calculating extinction times in a numerical simulation:

$$T(x_0) = \int_0^\infty \langle 1 - e^{-x} \rangle dt \quad (21)$$

Analytically, however, we can do better, and even find an exact solution just requiring numerical integration.  $\mathcal{J}$  is a linear functional of the Poisson distribution  $f(t, x|x_0)$ , and as such must satisfy the well-known “backward” Kolmogorov equation<sup>9</sup> in terms of its initial condition:

$$\frac{d}{dt} \mathcal{J}(tx_0) = \left[ A(x_0) \partial_{x_0} + \frac{1}{2} D(x_0) \partial_{x_0}^2 \right] \mathcal{J}(tx_0) \quad (22)$$

We can now integrate the above equation over all times to obtain an ordinary differential equation for  $T(x_0)$ . Initially,  $\mathcal{J}(0|x_0) = 1 - e^{-x_0}$  so that

$$\begin{aligned}\mathcal{J}(\infty|x_0) - \mathcal{J}(0|x_0) &= e^{-x_0} - 1 \\ &= \left[ A(x_0) \partial_{x_0} + \frac{1}{2} D(x_0) \partial_{x_0}^2 \right] T(x_0)\end{aligned}\quad (23)$$

We note that the mean extinction time must vanish at  $x = 0$ . Under this innate boundary condition the differential equation above yields the particular solution:

$$T(x_0) = 2 \int_0^{x_0} \frac{dx}{D(x) \psi(x)} \int_x^{x_m} \psi(z) (1 - e^{-z}) dz \quad (24)$$

Here we have introduced the auxiliary function,

$$\begin{aligned}\psi(x_0) &= \frac{2}{D(x_0)} \exp \left[ \int_{x_0}^{x_m} \frac{2A(x)}{D(x)} dx \right] \\ &= \frac{1}{x_0(k'_1 - k_2 x_0)} \exp \left[ \int_{x_0}^{x_m} \left( 1 - \frac{\gamma}{k'_1 - k_2 x} \right) dx \right] \\ &= \frac{e^{x_0}}{x_0} (k'_1 - k_2 x_0)^{\gamma/k_2 - 1}\end{aligned}\quad (25)$$

This solution satisfies the backward Kolmogorov equation, and the boundary condition at  $x = 0$ . In principle, another solution

**TABLE 1: Comparison between Analytically Obtained Exact Values for the Mean Extinction Time and Those Obtained Numerically via Gillespie’s Stochastic Simulation Algorithm (SSA), for  $k'_1 - \gamma = 1$**

$\rho$	$N_c$	$T(x_0 = N_c)$	
		analytical	SSA <sup>a</sup>
1.2	5	1.820	1.821 ± 0.002
1.5	5	4.587	4.583 ± 0.004
2.0	5	10.126	10.13 ± 0.01
3.5	5	32.91	32.97 ± 0.03
6.0	5	83.92	83.95 ± 0.08
1.2	10	3.996	3.990 ± 0.004
1.5	10	12.86	12.84 ± 0.01
2.0	10	41.22	41.27 ± 0.04
3.5	10	291.3	291.5 ± 0.3
6.0	10	1430	1431 ± 1.4
1.2	20	10.60	10.60 ± 0.01
1.5	20	66.03	66.06 ± 0.06
2.0	20	593.9	589.7 ± 1.9*
3.5	20	$2.835 \times 10^4$	$2.825 \times 10^4 \pm 89^*$
6.0	20	$5.884 \times 10^5$	$5.936 \times 10^5 \pm 6.0 \times 10^3^{**}$

<sup>a</sup> Note that all SSA results were obtained by averaging over  $10^6$  trajectories, with the exception of those marked \* and \*\* for which reduced ensemble sizes of respectively  $10^5$  and  $10^4$  were used.

is possible, as the differential equation is of second order. However, eq 23 has a regular singular point at  $x = x_m$ , whose indicial equation indicates that any other independent solution of the homogeneous equation would be singular at  $x = x_m$ , and hence inadmissible.

Our result is remarkably similar to the standard expression for a first-passage time of a diffusion process<sup>9</sup> except for the factor of  $(1 - e^{-z})$  in the integrand. This has the simple intuitive interpretation that it projects out the fraction of the population in a given Poisson ensemble that has not yet reached extinction. While this term is essential if an exact result is required, it is typically a small correction in an expression dominated by the exponential factors in  $\psi$ .

Extinction time results for a range of parameter values are given in Table 1, alongside results obtained via Gillespie’s stochastic simulation algorithm.<sup>28</sup> These two sets of results agree to within two standard deviations of the computational sampling error in all cases. This provides strong numerical evidence for the accuracy of our analytical result. Numerical integrations of eq 24 were checked for accuracy to at least four significant figures, using an adaptive routine (tolerance of  $0.5 \times 10^{-6}$ ) for the outer integral and a fixed step integration with  $4 \times 10^3$  steps of the  $z$  variable.

**Effective Potential Approximation.** To encourage an intuitive understanding of the mechanism behind these noise-driven extinction events, we now develop an approximate form of the exact result just derived.

We begin by considering a new continuous variable  $y$  whose dynamics are driven by a stochastic diffusion process according to the FPE

$$\frac{\partial}{\partial t} p(y, t) = \frac{\partial}{\partial y} U'(y) p(y, t) + \frac{\partial^2}{\partial y^2} p(y, t) \quad (26)$$

Here  $U'(y) = (\partial/\partial y)U(y)$  where  $U(y)$  is the potential function that governs the deterministic motion of the process. Placing an artificial reflecting boundary at  $y = y_m$  where  $y_m \in \mathbb{R}^+$  and a similarly artificial absorbing boundary at the origin restricts the dynamics to the domain  $[0, y_m]$ . According to established

theory,<sup>9</sup> the mean first passage time to the absorbing state at the origin for this process is given by

$$T(y_0) = 2 \int_0^{y_0} dy e^{U(y)} \int_y^{y_m} dY e^{-U(Y)} \quad (27)$$

We now propose a relationship between the Poisson representation variable  $x$  and the new stochastic variable  $y$ , by defining  $dx/dy = [D(x)]^{1/2}$ . This allows us to rewrite the expression for the mean extinction times of the autocatalytic reagent population in the following way:

$$T(x_0) = 2 \int_0^{y_0} \frac{dy}{\sqrt{D(x)} \psi(x)} \int_y^{y_m} \sqrt{D(z)} \psi(z) (1 - e^{-z}) dz \quad (28)$$

Here we have defined  $y_0 = y(x_0)$ ,  $y_m = y(x_m)$  and have made use of the short-hand notation  $x \equiv x(y)$  and  $z \equiv z(Y)$ . (The fact that  $[D(x)]^{1/2} \geq 0$  for  $x \in [0, x_m]$  means that the mapping  $x(y)$  is one-to-one, further implying that the inverse mapping  $y(x)$  is also uniquely defined.)

From eq 25 we see that the product  $[D(x)]^{1/2} \psi(x)$  is given explicitly by

$$\sqrt{D(x)} \psi(x) = e^x \sqrt{\frac{2}{x}} (k'_1 - k_2 x)^{\gamma/k_2 - (1/2)} \quad (29)$$

which possesses turning points at

$$x^\pm = \frac{1}{2}(N_c + 1) \left( 1 \pm \sqrt{1 - \frac{2x_m}{(N_c + 1)^2}} \right) \quad (30)$$

where  $x^+$  is a local maximum and  $x^-$  a local minimum. When  $N_c \gg (2x_m)^{1/2}$  the local maximum will dominate the inner integral in eq 28, meaning that in that case one can neglect the exponential factor  $(1 - e^{-z})$ . Using the formal equivalence of the resulting expression to eq 27 we define the following effective potential function

$$\begin{aligned} U(y) &= -\log[\sqrt{D(x)} \psi(x)] \\ &= -x + \frac{1}{2} \log \left[ \frac{x}{2} (k'_1 - k_2 x)^{1-2\gamma/k_2} \right] \end{aligned} \quad (31)$$

where we have again used the notation  $x \equiv x(y)$ . Note that, in terms of  $x$ , the positions of the extrema are again given by eq 30, although their roles are reversed:  $U^- \equiv U(y(x^-))$  is a local maximum and  $U^+ \equiv U(y(x^+))$  a local minimum.

The general form of this distribution as illustrated in Figure 2 for the parameter values  $k'_1 = 10$ ,  $k_2 = 1$ , and  $\gamma = 3$  offers a nicely intuitive interpretation of the behavior of the autocatalytic population as it nears extinction. Initially, finite populations tend to localize about the metastable fixed point at  $x^\pm \approx N_c$ , where they are temporarily confined between the singularity at  $x_m$  and the finite potential barrier centered on the local maximum at  $x^-$ . Inevitably, however, fluctuations drive the populations over the potential barrier to extinction.

At this juncture, it is instructive to compare the effective potential derived here from the stochastic description of the kinetic model with that given earlier in eq 3 and shown for an equivalent set of rate parameters as the dashed line in Figure 1,

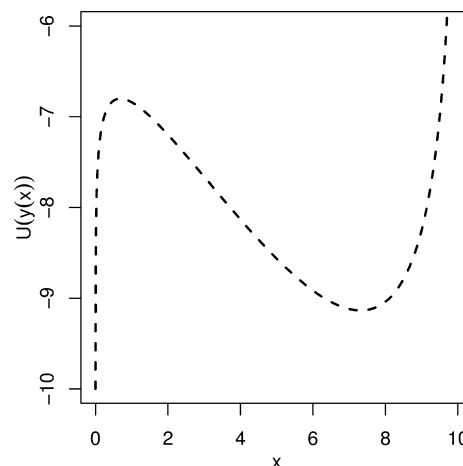


**Figure 2.** Form of the effective potential for a system with the parameters  $k'_1 = 10$ ,  $k_2 = 1$ , and  $\gamma = 3$ . (For these parameters  $x_m = 10$ .)

which was obtained from the traditional deterministic rate equation description. Both potentials possess minima for finite values of the autocatalytic population, although for the stochastic potential this minimum is shifted slightly away from the origin (as  $x^+ > N_c$  in this case). However, the most striking difference is at the origin where both systems possess a stationary point. As noted previously, this point corresponds to a local maximum in the deterministic potential (for  $\rho > 1$ ) and is thus unstable. In contrast, the equivalent point on the stochastic potential approaches  $-\infty$ . This implies that not only does the origin become a stable stationary point in this case but also the discrete nature of the population and the associated stochastic fluctuations cause the origin to usurp the role of the finite population minimum and become the location of the system's *global* potential minimum.

Provided that the extrema of the effective potential are well separated, a condition satisfied when  $N_c \gg (2x_m)^{1/2}$ , the expression for the extinction time in terms of the effective potential in eq 27 can be further approximated using standard techniques.<sup>9</sup> These involve noting first that the integrands  $\exp[-U(y)]$  and  $\exp[U(y)]$  are sharply peaked at disparate locations under the given conditions, meaning that the integrals can be effectively decoupled:

$$T(x_0) \approx \left( \int_0^{y_0} dy e^{U(y)} \right) \left( \int_0^{y_m} dY e^{-U(Y)} \right) \quad (32)$$

We then construct the following local second-order approximations for the effective potential:

$$U_{(-)}(y) \approx U^- + \frac{\kappa_-}{2} (y - y^-)^2 \quad (33)$$

$$U_{(+)}(y) \approx U^+ + \frac{\kappa_+}{2} (y - y^+)^2 \quad (34)$$

where we have used the curvatures

$$\begin{aligned} \kappa_\pm &\equiv \frac{d^2 U(y^\pm)}{dy^2} = D(x^\pm) \frac{d^2}{dx^2} U(y^\pm) \\ &= \pm k_2 \sqrt{(N_c + 1)^2 - 2x_m} \equiv \pm \kappa \end{aligned} \quad (35)$$



Substituting  $U_{(-)}(y)$  and  $U_{(+)}(y)$  into the first and second integrals of eq 32, respectively, transforms the integrands into simple Gaussian functions.

Finally, we acknowledge that for  $x_0 \gg x^-$  the precise location of the upper bound on the domain of the first integral is unimportant and can, to good approximation, be replaced by  $+\infty$ . Likewise, the lower bound on the domain of the second integral can be replaced by  $-\infty$ . These modifications allow the integrals to be evaluated analytically, yielding

$$T(x_0 \gg x^-) \approx \frac{2\pi}{\kappa} \exp[U^- - U^+] \quad (36)$$

This is analogous to the inverse of the usual Arrhenius expression for the rate at which a chemical reaction occurs. The difference between the maximum and minimum effective potential energies can therefore be regarded as an activation energy for an effective reaction linking the metastable state at  $x^+ \sim N_c$  to the state in which the autocatalytic population has become extinct.

## Discussion

Thus far we have demonstrated how the Poisson representation can be used to derive solutions to the extinction time problem of a reversible autocatalytic process subject to degradation. In this section, we briefly discuss some qualitative features of these times, paying special attention to the influence exerted by finite temperature effects. We also discuss the potential for experimental implementations of this model to undergo destructive autocatalytic runaway.

**Limiting Behavior.** First, we consider an asymptotic form of mean extinction time expression given in eq 36 in the limit that the critical number  $N_c$  far exceeds the maximum mean population size  $x_m = k'_1/k_2$ . (Note that this is the same limit in which the last approximation is valid, but here we take the approximation further.) We obtain this by first noting that, in this limit, the turning points of the effective potential approach

$$x^+ \sim N_c + 1 - \frac{k'_1}{2(k'_1 - \gamma)} \quad (37)$$

$$x^- \sim \frac{k'_1}{2(k'_1 - \gamma)} \quad (38)$$

Substituting these values into eq 36 we find to leading order in  $N_c$  that the extinction time is

$$T \sim T_0 \exp\left[N_c \left(1 - \frac{\log \rho}{\rho - 1}\right)\right] \quad (39)$$

where we have again used  $\rho = k'_1/\gamma$  and have introduced the fundamental extinction time scale

$$T_0 = \frac{2\pi\rho}{(k'_1 - \gamma)} \sqrt{\frac{1}{2eN_c(\rho - 1)}} \quad (40)$$

Extinction times obtained using this asymptotic expression are illustrated in Figure 3, where they are graphed against  $\rho$  for a variety of  $N_c$  and with  $k'_1 - \gamma$  fixed to 1 (i.e., the same combination of parameters used to produce Table 1). The

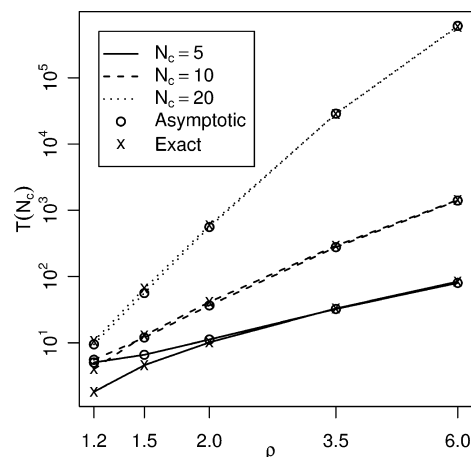


**Figure 3.** Comparison of extinction times obtained via the asymptotic expression with the exact results. Parameter combinations are the same as those used in Table 1.

corresponding exact results are also displayed for comparison, demonstrating that the approximation does quite well provided that  $N_c$  is large, as anticipated.

From the approximate expression given as eq 39 it is manifestly clear that, although the extinction time increases exponentially with the increasing critical population size  $N_c$ , there is also an exponential dependence on the ratio  $\rho = k'_1/\gamma$ . This additional dependence can result in strong reductions in the extinction time *even when the deterministically stable population size is very large*. This can occur, for example, if the difference  $k'_1 - \gamma$  is large in absolute terms and yet small in comparison to the magnitude of either  $k'_1$  or  $\gamma$ , meaning that  $k'_1/\gamma$  is close to unity. This effect is due to the presence of large intrinsic fluctuations in systems with closely matched rates for the forward reaction and the decay process, which quickly drive such systems over the effective potential barrier separating the metastable state from the extinct state.

The limiting behavior of the extinction times also delivers a simple means of highlighting those regions of parameter space for which the deterministic rate equations provide an adequate (at least in the short term) description of the dynamics of the ensemble-averaged autocatalytic population size. This is done by defining a critical average extinction time,  $T_c$ , above which systems can be considered essentially deterministic. In practice, the critical value chosen should be set by the maximum time frame of an experiment. However, to obtain a qualitative understanding of the parameter space regions so defined we define  $T_c = 100T_0$ , with  $T_0$  being the fundamental extinction time scale defined above. Noting that the relative asymptotic extinction time  $T/T_0$  is solely a function of  $N_c$  and  $\rho$ , the parametric demarcation thus obtained is illustrated in Figure 4, where the regions satisfying  $T/T_0 > 100$  and  $T/T_0 < 100$  have been respectively labeled “deterministic” and “stochastic”. [This visualization approach was inspired by the recent work of Lente.<sup>32</sup>]

The hyperbolic shape of the boundary in this figure clearly illustrates the fact stated above that *both* the critical population size  $N_c$  and the birth/death ratio  $\rho$  must be large to delay the impact of noise-driven extinction events. In particular, we again see that unless the forward reaction rate  $k'_1$  is significantly larger than the X decay rate  $\gamma$ , even very large metastable populations are likely to be rapidly eliminated.

**Autocatalytic Runaway.** As noted earlier in the paper, the stochasticity of the model implies that there is always a finite



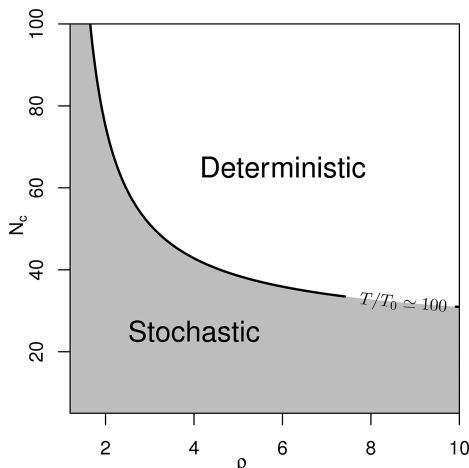


**Figure 4.** Illustration of the parameter space regions that exhibit manifestly stochastic and deterministic dynamics, defined in terms of the expected lifetime of the metastable state.

probability that the autocatalytic population will violate the requirement that  $N_X \ll N_Y$ . We now consider this problem in more detail.

To gauge the probability of an autocatalytic runaway event, defined here as a fluctuation of the autocatalytic population, we define a critical magnitude  $N_X^{(R)}$ . The runaway probability can then be defined as the probability of the population exceeding this threshold at any time during the progress of the reaction.

Rather than calculating this probability directly, we focus here on fixing an absolute upper bound on the maximum rate at which, for an ensemble of identically conditioned experiments, the autocatalytic populations within individual experiments can be expected to exceed  $N_X^{(R)}$ . By comparing this upper limit to the minimum rate at which these same experiments can be expected to instead become extinct, we can gauge the degree to which runaway events are a practical impediment to validity of our model for a given critical magnitude.

We begin by considering that the extinction rate given in eq 16 can also be written

$$\frac{d}{dt} \mathcal{E}(tx_0) = \gamma \int_0^{x_m} dx f(x, tx_0) e^{-x} x \quad (41)$$

recalling that  $\mathcal{E}(tx_0)$  represents the probability that an extinction event has occurred by time  $t$ . Similarly, the rate at which runaway events occur can be expressed as

$$\frac{d}{dt} \mathcal{R}(tx_0) = k'_1 N_X^{(R)} \int_0^{x_m} dx f(x, tx_0) e^{-x} \frac{x^{N_X^{(R)}}}{N_X^{(R)}!} \quad (42)$$

where we have used  $\mathcal{R}(tx_0)$  to denote the probability that a runaway event has occurred by time  $t$ . Calculation of the bounds on these rates are facilitated by the fact that, as noted previously, the Poisson representation variable  $x$  is constrained to satisfy  $0 \leq x \leq x_m$  for all  $t > 0$  when it is initialized according to a Poissonian probability distribution  $P(n, 0|x_0) = \exp[-x_0] x_0^n / n!$  with the mean satisfying  $x_0 \in [0, x_m]$ . For a given survival probability  $\mathcal{J}(tx_0) \equiv 1 - (\mathcal{E}(tx_0) + \mathcal{R}(tx_0))$ , the maximum possible runaway rate is obtained when the nonextinct probability distribution is concentrated at  $x_m$ , ensuring that the following inequality is satisfied:

$$\frac{d}{dt} \mathcal{R}(tx_0) \leq \mathcal{J}(tx_0) k'_1 e^{-x_m} x_m^{N_X^{(R)}} / N_X^{(R)}! \quad (43)$$

Likewise, for the same survival probability, the *minimum* possible extinction rate is obtained via the same Poissonian distribution, yielding

$$\frac{d}{dt} \mathcal{E}(tx_0) \geq \mathcal{J}(tx_0) \gamma e^{-x_m} x_m \quad (44)$$

Taken together, these inequalities fix an absolute upper bound on the ratio of the runaway rate to the extinction rate. That is,

$$\frac{\mathcal{R}(tx_0)}{\mathcal{E}(tx_0)} \leq \phi_{N_X^{(R)}}(x_m) \quad (45)$$

where

$$\phi_{N_X^{(R)}}(x_m) = \rho \frac{x_m^{(N_X^{(R)}-1)}}{(N_X^{(R)}-1)!} \quad (46)$$

is the upper bound. (The dots above the runaway and extinction probabilities represent time derivatives.) As the value of  $x_m$ , representing an absolute number of reactant particles, will likely be large in practice, this unnormalized Poissonian distribution can be replaced by a Gaussian approximation to yield

$$\phi_{N_X^{(R)}}(x_m) \approx \rho \frac{e^{x_m}}{\sqrt{2\pi x_m}} \exp[-(N_X^{(R)} - 1 - x_m)^2 / 2x_m] \quad (47)$$

Defining  $\alpha = N_X^{(R)} / x_m$ , this becomes

$$\begin{aligned} \phi_{\alpha x_m}(x_m) &\approx \frac{\rho}{\sqrt{2\pi x_m}} \exp\left[\frac{-((\alpha - 1)x_m - 1)^2}{2x_m} + x_m\right] \\ &\approx \frac{\rho}{\sqrt{2\pi x_m}} \exp\left[-x_m\left(\frac{1}{2}(\alpha - 1)^2 - 1\right)\right] \end{aligned} \quad (48)$$

For  $N_X^{(R)}$  as low as  $3x_m$  we find that the maximum runaway rate is strictly constrained to be *exponentially* lower than the minimum possible extinction rate:

$$\phi_{3x_m}(x_m) \approx \frac{\rho}{\sqrt{2\pi x_m}} e^{-x_m} \quad (49)$$

We therefore find that, while destructive runaway of the autocatalytic population is a real concern, it will be exceedingly rare in practice, provided that the stability of the noncatalytic reagent population can be maintained for  $X$  population sizes  $N_X \lesssim x_m$ .

To gauge the validity of this analytical result, Gillespie's stochastic simulation algorithm was used to numerically calculate the probability with which a system initialized with a Poissonian distribution centered on the deterministic stationary population size (the carrying capacity  $N_c$ ) can be expected to

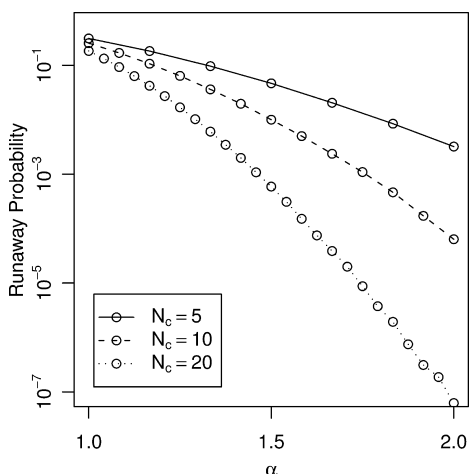


**Figure 5.** Numerically calculated runaway probabilities for  $\rho = 6$ ,  $N_c = 5, 10$ , and  $20$  and a variety of relative runaway thresholds  $\alpha = N_X^{(R)}/x_m$ . Note the superexponential decay of these probabilities with increasing  $\alpha$ .

exceed the runaway threshold  $N_X^{(R)} = \alpha x_m$  at some time prior to extinction. Calculations were performed for each of a variety of runaway thresholds and reaction rates, and the results, which are presented in Figure 5, clearly demonstrate that the probability of autocatalytic runaway rapidly becomes negligible in all cases.

**Finite Temperature Effects.** While we have chosen to represent the reaction rates  $k_1$ ,  $k_2$ , and  $\gamma$  as constants in our mathematical model, it is interesting to note that in reality these rates are highly dependent on many aspects of the environment in which the reactions are actually taking place. In particular, each of these rates is governed by an Arrhenius formula that gives an explicit temperature dependence in terms of the activation energy of that reaction:

$$k_1(\beta) = k_1(0) \exp[-\beta E_1] \quad (50)$$

$$k_2(\beta) = k_2(0) \exp[-\beta E_2] \quad (51)$$

$$\gamma(\beta) = \gamma(0) \exp[-\beta E_3] \quad (52)$$

Here  $\beta = 1/k_B T$  is the inverse temperature and  $E_i$  are the activation energies of the three reactions involved in our model. [One might argue that eqs 50–52 are invalid in this context as the Arrhenius equation applies only to elementary chemical reactions while all known examples of autocatalytic reactions are composite reactions. However, the rates of such reactions are often dominated by that of a single elementary reaction for which the Arrhenius equation yields the correct temperature dependence.]

In terms of these temperature-dependent rates, the critical population size can be written

$$N_c(\beta) = \frac{k_1'(0)e^{\beta(E_2-E_1)} - \gamma(0)e^{\beta(E_2-E_3)}}{k_2(0)} \quad (53)$$

and the ratio  $\rho$  can be written

$$\rho(\beta) = \frac{k_1'(0)}{\gamma(0)} e^{\beta(E_3-E_1)} \quad (54)$$

Assuming that the forward and reverse autocatalytic process have respectively the lowest and highest activation energies, and assuming furthermore that the activation energy of the decay process lies somewhere between these, both the critical population size and  $\rho$  will be increasing functions of  $\beta$ . Given the relationship presented in eq 39, we therefore expect extinction times of autocatalytic populations to lengthen superexponentially as the temperature of the system is reduced.

## Summary

In any real autocatalytic system, decay of the autocatalytic reagent population has the potential to play an important role. In particular, decay processes can lead to the irreversible extinction of the autocatalytic reagent population whenever the uncatalyzed production of that population is sufficiently rare. In this paper we have demonstrated that the Poisson representation can be used to derive exact predictions for the mean time to extinction for autocatalytic systems evolving under a stochastic model of the chemical dynamics. We have used an approximation to these exact predictions to show that the mechanism behind the transition of the population from its metastable state to extinction is similar to that of the familiar Arrhenius model of reaction dynamics.

Additionally, we have investigated the asymptotic behavior of this approximation and have shown that intrinsic fluctuations can drive autocatalytic reagent populations to extinction very rapidly, especially when the rates of the forward reaction and the decay process are closely matched. This striking feature of the stochastic dynamics directly results from the inclusion of the decay process and is likely to have important practical implications.

Also, to gauge the potential for noise-driven autocatalytic runaway in real experimental implementations of this model, we have calculated an upper bound on the ratio of the rate at which autocatalytic populations exceed a given upper bound to the rate at which those same populations become extinct. We found that this upper bound is an exponentially decreasing function of the runaway threshold and that such runaway events could be neglected from consideration provided that the population of the noncatalytic precursor  $Y$  could be held stable for autocatalytic population sizes satisfying  $N_X \lesssim k_1'/k_2$ .

Finally, we have briefly discussed the possible effects of temperature variation on the extinction times. Although more careful analysis, including use of the true effective activation energies for each of the relevant processes, should be undertaken, our initial investigation has indicated that extinction times may increase very rapidly (superexponentially) as the temperature of a reacting system is lowered. This suggests that low operating temperatures may be important for the persistence of autocatalytic populations when these populations are subject to decay.

**Acknowledgment.** We thank Peter Wills of the University of Auckland for useful and stimulating discussions. We also gratefully acknowledge the helpful suggestions of two anonymous reviewers. This work was supported by the Australian Research Council through a Discovery Project Grant (DP0773445).

## References and Notes

- (1) Paul, N.; Joyce, G. F. *Proc. Natl. Acad. Sci. U.S.A.* **2002**, *99*, 12733–12740.
- (2) Lee, D. H.; Granja, J. R.; Martinez, J. A.; Severin, K.; Ghadri, M. R. *Nature* **1996**, *382*, 525.
- (3) Eigen, M. *Biophys. Chem.* **1996**, *63*, A1.
- (4) Witzemann, E. J. *J. Phys. Chem.* **1924**, *28*, 305.

- (5) Plasson, R.; Kondepudi, D. K.; Bersini, H.; Commeyras, A.; Asakura, K. *Chirality* **2007**, *19*, 589.
- (6) Issac, R.; Chmielewski, J. *J. Am. Chem. Soc.* **2002**, *124*, 6808.
- (7) Guldberg, C.; Waage, P. C. M. *Forhandlinger: Videnskabs-Selskabet i Christiana* **1864**, 35.
- (8) Guldberg, C. C. M. *Forhandlinger: Videnskabs-Selskabet i Christiana* **1864**, 111.
- (9) Gardiner, C. W. *Handbook of Stochastic Methods for Physics, Chemistry and the Natural Sciences*, 3rd ed.; Springer-Verlag: Berlin, Heidelberg, New York, 2004.
- (10) Delbrück, M. *J. Chem. Phys.* **1940**, *8*, 120.
- (11) Kramers, H. *Physica* **1940**, *7*, 284.
- (12) Moyal, J. J. R. *Stat. Soc., Ser. B* **1949**, *11*, 150.
- (13) van Kampen, N. G. *Can. J. Phys.* **1961**, *39*, 551.
- (14) Gaveau, B.; Moreau, M.; Tóth, J. *Lett. Math. Phys.* **1996**, *37*, 285.
- (15) Gardiner, C. W.; Chaturvedi, S. *J. Stat. Phys.* **1977**, *17*, 429.
- (16) Chaturvedi, S.; Gardiner, C. W. *J. Stat. Phys.* **1978**, *18*, 501.
- (17) Arslan, E.; Laurenzi, I. J. *J. Chem. Phys.* **2008**, *128*, 015101.
- (18) Podlech, J. *Cell. Mol. Life Sci.* **2001**, *58*, 44.
- (19) Frank, F. C. *Biochim. Biophys. Acta* **1953**, *11*, 459.
- (20) Soai, K.; Shibata, T.; Morioka, H.; Choji, K. *Nature* **1995**, *378*, 767.
- (21) Saito, Y.; Hyuga, H. *J. Phys. Soc. Jpn.* **2004**, *73*, 33.
- (22) Lente, G. *React. Kinet. Catal. Lett.* **2008**, *95*, 13.
- (23) Näsell, I. J. *Theor. Biol.* **2001**, *211*, 11.
- (24) Paul, N.; Joyce, G. F. *Curr. Opin. Chem. Biol.* **2004**, *8*, 634.
- (25) Verhulst, P. *Corresp. Math. Phys.* **1838**, *10*, 113.
- (26) Newman, T. J.; Ferdy, J.-B.; Quince, C. *Theor. Popul. Biol.* **2004**, *65*, 115.
- (27) Gillespie, D. T. *J. Comput. Phys.* **1976**, *22*, 403.
- (28) Gillespie, D. T. *J. Phys. Chem.* **1977**, *81*, 2340.
- (29) Lente, G. *J. Phys. Chem. A* **2004**, *108*, 9476.
- (30) Lente, G. *J. Phys. Chem. A* **2005**, *109*, 11058.
- (31) Lente, G. *J. Phys. Chem. A* **2006**, *110*, 12711.
- (32) Lente, G. *Phys. Chem. Chem. Phys.* **2007**, *9*, 6134.
- (33) Saito, Y.; Sugimori, T.; Hyuga, H. *J. Phys. Soc. Jpn.* **2007**, *76*, 044802.
- (34) Cruz, J. M.; Parmananda, P.; Buhse, T. *J. Phys. Chem. A* **2008**, *112*, 1673.
- (35) Lente, G.; Ditrói, T. *J. Phys. Chem. B* **2009**, *113*, 7237.
- (36) Lente, G. *Symmetry* **2010**, *2*, 767.
- (37) van Kampen, N. G. *Stochastic Processes in Physics and Chemistry*, 3rd ed.; Elsevier: Amsterdam, Boston, Heidelberg, 2007.
- (38) Voiturie, R.; Moreau, M.; Oshanin, G. *J. Chem. Phys.* **2005**, *122*, 084103.
- (39) Gopich, I. V.; Szabo, A. *Chem. Phys.* **2002**, *284*, 91.
- (40) de Pasquale, F.; Mecozzi, A. *Phys. Rev. A* **1984**, *31*, 2454.

JP104471E